Published online July 2, 2018

Original Research

Core Ideas

- The stochasticity of 3D root architecture models needs to be recognized by statistical analysis.
- Probability density functions, regression, and correlation analyses reveal the impact of model input parameters on different CRootBox measures.
- Distributions of ratios of root system measures are highly asymmetric.
- Multivariate approaches (copulas) are envisioned for future root architecture model analysis.

Statistical Characterization of the Root System Architecture Model CRootBox

A. Schnepf,* K. Huber, M. Landl, F. Meunier, L. Petrich, and V. Schmidt

The connection between the parametrization of three-dimensional (3D) root architecture models and characteristic measures of the simulated root systems is often not obvious. We used statistical methods to analyze the simulation outcome of the root architecture model CRootBox and built meta-models that determine the dependency of root system measures on model input parameters. Starting with a reference parameter set, we varied selected input parameters one at a time and used CRootBox to compute 1000 root system realizations as well as their root system measures. The obtained data sets were then statistically analyzed with regard to dependencies between input parameters, as well as distributions and correlations between different root system measures. While absolute root system measures (e.g., total root length) were approximately normally distributed, distributions of ratios of root system measures (e.g., root tip density) were highly asymmetric and could be approximated with inverse gamma distributions. We derived regression models (meta-models) that link significant model parameters to 18 widely used root system measures and determined correlations between different root system measures. Statistical analysis of 3D root architecture models helps to understand the impact of input parametrization on specific root architectural measures. Our developed meta-models can be used to determine the effect of parameter variations on the distribution of root system measures without running a full simulation. Model intercomparison and benchmarking of root architecture models is still missing. Our approach provides a means to compare different models with each other and with experimental data.

Abbreviations: 3D, three-dimensional; HMD, half mean distance; KDE, kernel density estimator; SUF, standard root water uptake fraction.

A. Schnepf, K. Huber, and M. Landl, Institut für Bio- und Geowissenschaften: Agrosphäre (IBG-3), Forschungszentrum Jülich GmbH, Wilhelm-Johnen-Str., D-52425 Jülich, Germany; F. Meunier, Earth and Life Institute, Univ. Catholique de Louvain, 15-de Serres, Croix du Sud 2, 1348 Louvain-la-Neuve, Belgium; L. Petrich and V. Schmidt, Institute of Stochastics, Ulm Univ., Helmholtzstr. 18, D-89069 Ulm, Germany. *Corresponding author (a.schnepf@fz-juelich.de).

Received 12 Dec. 2017.
Accepted 30 Apr. 2018.

Citation: Schnepf, A., K. Huber, M. Landl, F. Meunier, L. Petrich, and V. Schmidt. 2018. Statistical characterization of the root system architecture model CRootBox. Vadose Zone J. 17:170212. doi:10.2136/vzj2017.12.0212

Root architecture and phenotypic plasticity determine a plant's success to acquire belowground resources such as water and nutrients (Lynch, 2007). Experimental investigation of root system development, however, is a laborious task due to the opaque nature of the soil that makes direct measurements difficult. Researchers therefore usually resort to simplified experimental designs and derive root system measures from plants grown in artificial systems such as hydroponics or rhizotron boxes (Nagel et al., 2015; Atkinson et al., 2015) or from observations through rhizotubes in the field, where only small sections of the root system are visible (Garré et al., 2012). Several studies, however, showed that laboratory and field-derived phenotypic root properties are poorly related, and extrapolation from single root observations to the entire root system is delicate (Wojciechowski et al., 2009; Poorter et al., 2016).

A possibility to overcome these limitations is provided by three-dimensional (3D) root architecture models, which allow large numbers of different root systems to be generated from a range of plant-specific and environmentally influenced input parameter sets (Schnepf et al., 2018), which can then be used to deduce characteristic root traits. Models of root architecture and function have become readily available (Dunbabin et al., 2002; Schnepf et al., 2018; Postma et al., 2017; Pagès et al., 2014) and provide a means to efficiently analyze different plant species and their performance in different environments (Meunier et al., 2016). Most models use comparable input parameter sets that include parameters influencing the total size of a root system (e.g., growth speed, branching density)

as well as the shape of a root system (e.g., tropism and tortuosity parameters) (Bingham and Wu, 2011). Furthermore, most models have stochastic components such that the same parameter set may produce many different realizations. However, to our knowledge, none of these models has so far been subject to thorough statistical analysis regarding the dependence of root system measures on model parameterization. We chose a terminology that explicitly distinguishes between the "model input parameters," from which we compute the 3D root architecture using CRootBox, and statistical "measures," which we compute from the resulting 3D root architecture. Both could be ecological "traits." For example both the model input parameter "branching angle" and the "root length density" could be considered traits.

Measures to Characterize Root Architectures

Classical measures to characterize root system architectures include total root length, root surface area, and root volume. While total root length is related to the soil volume explored by the root system, root surface area is important for uptake and exudation mechanisms that occur across the root–soil interface, and root volume can be seen as a measure of carbon investment into a specific root structure. The number of branches (or number of root tips) gives information about the degree of branching within a root system. Maximum rooting depth and maximum horizontal spread of the root system are negatively correlated and determine whether the root system is of steep and deep (Lynch, 2013) or of shallow appearance, which has direct implications on root foraging. While deep-rooting plants can take up water from deeper soil layers and are thus advantageous in dry climates and during drought periods, shallow-rooting plants enhance the exploration of topsoil layers, where nutrient availability is greatest in many soils (Lynch and Brown, 2001). Irrespective of the specific location, the convex hull determines the smallest convex set that encloses the whole root system, while the rhizosphere volume is a measure of the soil volume that is actually influenced by the root system. The size of the rhizosphere volume depends on the effective soil diffusion coefficient, which varies for different nutrients, as well as by root age, root length and radius, and overlap between rhizospheres of individual root axes, i.e., the foraging performance (Landl et al., 2018).

To compare root systems of different plant species with each other, ratios of root system measures are used. Normalizing the number of root tips, total root length, root surface area, and root volume by the volume of the convex hull results in root tip density, root length density, root surface area density, and root volume density. We chose the convex hull because our simulations refer to the root system of a single plant. Under field conditions, the volume of the convex hull would be replaced by the volume of the sampled soil and, potentially, root systems from several plants would contribute to the root system measures. While root length density is one of the most widely measured traits in many laboratory or field experiments (Zuo et al., 2004; van Noordwijk et al., 1985), root surface area density is the most relevant parameter in water flow and solute transport models (Couvreur et al., 2014).

Root water and nutrient uptake as well as transport toward the shoot is determined by root hydraulic properties, which are thus—next to root architecture parameters—key components for root system functioning (Vadez, 2014). To describe the hydraulic architecture of an entire root system, root hydraulic properties such as radial and axial conductivities are related to root system measures. Root hydraulic architecture measures include root system equivalent conductance (K_{rs}) and standard root water uptake fraction (SUF), which represent, respectively, the ability of the root system to take up a certain water volume under a given water potential difference between the root collar and an homogeneous soil and the water uptake by a root segment relative to the total water uptake of the root system. These variables were calculated by solving the water flow in the generated root system architectures under homogeneous soil conditions, using the algorithm of Meunier et al. (2017b). A water potential was imposed at the root collar and the resulting stem sap flow was used to calculate the root system conductance. The water uptake by each single segment served then to derive the standard uptake fraction of each individual segment. The root hydraulic conductivities (function of root age and order) were taken from Doussan et al. (2006) and considered as identical for all root systems. The mean depth of standard root water uptake is then the product of SUF and the depth of the respective root segment summed across all segments. To allow comparisons of the hydraulic architecture of differently sized root systems, the root system equivalent conductance is normalized by root length or root surface area (Couvreur et al., 2012). A further important measure for the characterization of root water uptake is the root half mean distance (HMD) which affects water depletion in the soil and is approximated with the classical approach of Newman (1969) as $HMD = (\pi RLD)^{-0.5}$, where RLD is the root length density. An overview of the different characteristic root system measures analyzed in this work is given in Table 1.

Statistical Tools to Analyze Characteristic Root System Measures from Root Architecture Model Outputs

Statistical methods have so far been mainly used to group different root systems into plant functional types (Bodner et al., 2013) or similar genotypes (Chen et al., 2017) based on principal component analysis. Furthermore, nonlinear least-square fitting has been used to fit model parameters based on modeled and measured root lengths in homogeneous root groups (Zhang et al., 2003). Bingham and Wu (2011) analyzed the effect of varying model input parameters on two root system measures, total root length and root distribution in the soil profile, in a sensitivity analysis. Pagès (2011) investigated the impact of different model input parameters as well as interactions between these parameters on the foraging performance of a root system.

The connection between the complex parameterization of 3D root architecture models and characteristic measures of the simulated root systems is often not obvious. Meta-models, which can

determine the effect of parameter variations on any of the different measures without running a full simulation, have recently been developed for root hydraulic measures (Meunier et al., 2017a); for root system measures, however, they are completely missing. To our knowledge, no stochastic root architecture model has so far been thoroughly analyzed with statistical methods.

Objectives

The objective of this work was to use statistical analysis methods to investigate the dependence of key root system measures on model input parameters using the example root architecture model CRootBox, which was chosen for its speed, efficiency, and flexibility as well as its acceptance within the root modeling community. For future work, it would, however, be beneficial to also apply the presented analysis methods to other root architecture models and even experimental data sets to allow comparisons of different simulators and validate dependencies between root system measures and model input parameters with experimental data.

In this study, we

- analyzed the distributions of characteristic measures of root architecture, e.g., maximum rooting depth with respect to model parameters of interest, e.g., initial growth speed
- derived statistical meta-models to link changes in individual model input parameters to the distributions of characteristic measures of root architecture, which will be helpful for CRootBox users to estimate the impact of a parameter change on the model's outcome
- elucidated correlations between different measures of root architecture
- computed the correlation changes between different architecture measures due to variations in individual model parameters

Table 1. Characteristic root system measures

Variable	Name and description
RL	total root length, cm
RSA	total root surface area, cm^2
RV	total root volume, cm^3
z_{max}	maximum rooting depth, cm
r_{max}	maximum horizontal spread (radius of the confining cylinder), cm
conv	volume of the convex hull, cm^3
NR	number of root tips or branches
V_{rhizo}	rhizosphere volume for phosphate, cm^3
RND	root tip density (NR/conv), cm^3
RLD	root length normalized by the volume of the convex hull (RL/conv), cm cm^{-3}
RSAD	root surface area normalized by the volume of the convex hull (RSA/conv), cm^2 cm^{-3}
RVD	root volume normalized by the volume of the convex hull (RV/conv), cm^3 cm^{-3}
VD_{rhizo}	rhizosphere volume for phosphate normalized by the volume of the convex hull (V_{rhizo}/conv), cm^3 cm^{-3}
K_{rs}	equivalent conductance of the root system, cm^2 d^{-1}†
$K_{rs\,A}$	equivalent conductance of the root system per unit root area (K_{rs}/RSA), d^{-1}
$K_{rs\,L}$	equivalent conductance of the root system per unit root length (K_{rs}/RL), cm d^{-1}
z_{SUF}	mean depth of standard root water uptake, cm
HMD	half mean distance between roots, cm

† $cm^2\ d^{-1} \cong cm^3\ hPa^{-1}\ d^{-1}$.

Materials and Methods

The Root Architecture Model CRootBox

CRootBox is a recent root architecture model (Schnepf et al., 2018). It is written in C++, but also has a Python binding that allows scripting in Python for most applications. Furthermore, a web application that is based on CRootBox enables the user to quickly create, modify, and export root architectures from a database that currently includes 22 plant species.

CRootBox is fully described in Schnepf et al. (2018). Briefly, it is a generic model that is not focused on a specific plant species but is able to simulate the root architectures of any monocotyledonous and dicotyledonous plant. It distinguishes different types of roots, i.e., tap roots, basal roots, shoot-borne roots, and lateral roots, and each root type is defined by a set of different model parameters. Basal and apical root zones define the length of the unbranched root before the first and behind the last branch, respectively. Branch spacing describes the distance between two successive branches and thereby determines branching density and the number of branches for a specified maximum root length. Root elongation is defined by a negative exponential function whose initial slope is determined by the initial growth speed (following the approach of Pagès et al., 2004) and whose asymptote is specified by the maximal root length. The insertion angle defines the angle from the vertical under which primary roots emerge (a larger angle thus leads to a more shallow root system), while the branching angle describes the initial angle between a branch and its parent root. The model is stochastic because of two aspects. First, the reorientation of a newly emerged root segment of defined length is determined by a random optimization algorithm that selects, from N randomly computed values of the deflection angle σ, the value with the closest proximity to the desired growth direction (tropism). For details, see Schnepf et al. (2018, Appendix A, section "Changes in root tip heading"). Second, all parameters are assumed to be normally distributed with user-defined mean and standard deviation. Thus, each realization of the same parameter set results in a different root system with variability depending on the standard deviations of the model input parameters, the type of tropism, and the random deflection angle σ. For our statistical analysis, we used the model parameters of the sample plant *Zea mays* (L.) as a reference data set. The parameter set was derived from the CRootBox model parameter database (Schnepf et al., 2018; Leitner et al., 2014) and is shown in Table 2. If the model structure remains the same, the dependence of root system measures on model input parameters is expected to remain qualitatively similar for different parameterizations, and the use of one single

Table 2. Model parameter set of *Zea mays* derived from the CRootBox model parameter database (Zea_maize_4_Leitner_2014) (Schnepf et al., 2018; Leitner et al., 2014).

Variable	Description	Axial roots	First-order laterals
l_b	basal root zone, cm	0.5 (0.5)†	0
l_a	apical root zone, cm	18.1 (1.81)	8.8
l_n	branch spacing, cm	0.5 (0.5)	1.2 (0.12)
l_{max}	maximum root length, cm	180.1 (18.01)	8.8
r	initial elongation rate, cm d^{-1}	2.94 (0.294)	0.75 (0.075)
a	root radius, cm	0.13 (0.013)	0.05 (0.005)
θ	insertion or branching angle, °	80 (8.0)	85 (8.5)
tropism N	number of additional trials	0.5	0.5
tropism σ	range of the random deflection angle, ° cm^{-1}	5.7	5.7
tropism type		gravitropism	exotropism
max_B	maximal number of basal roots	5	
simtime	simulation time, d	60	

† Standard deviations in parentheses.

reference parameter set is thus justified. As specified in the analysis below, we performed altogether 53,000 simulations of 3D root architectures based on the reference parameter set and its variations. A 3D visualization of a particular realization of this root system is shown in Fig. 1.

Analysis Methods

We selected six model input parameters from the reference parameter set in Table 2 that were expected to have diverse effects on root architecture development. For each of these six parameters, we chose a minimum and maximum value based on lower and upper parameter bounds of *Zea mays* found in literature (Leitner et al., 2010; Leitner et al., 2014; Pagès et al., 2014; Postma and Lynch, 2011). Standard deviations of the parameters were kept constant (Table 3). We then varied the means of each of the six parameters one at a time in four increments in the case of N, nine increments in the case of σ, and in 10 increments otherwise between the identified minimum and maximum value, resulting

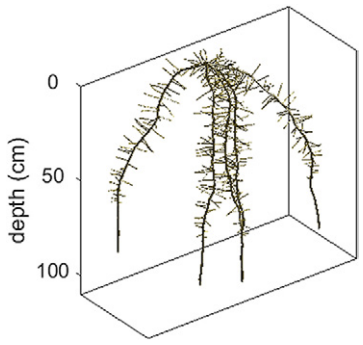

Fig. 1. Three-dimensional visualization of root architecture simulated by CRootBox using the reference parameter set of Table 1.

Table 3. Ranges of analyzed model input parameters of basal roots.

Model parameter	Reference	Min.	Max.
Axial root branch spacing (l_n), cm	0.5 (0.5)†	0.5 (0.5)	2 (0.5)
Maximal number of basal roots (max_B)	5	4	40
Initial elongation rate (r), cm d^{-1}	2.94 (0.294)	1 (0.294)	3 (0.294)
Range of random deflection angle (σ), ° cm^{-1}	5.7	0	5.7
Insertion or branching angle (θ), °	80 (8.0)	40 (8.0)	85 (8.0)
Number of additional trials (N)	0.5	0	2

† Standard deviations in parentheses.

in 53 different parameter sets altogether. Subsequently, we used CRootBox to simulate $n = 1000$ root system realizations for each of the 53 parameter sets and computed their characteristic root system measures (Table 1). Figure 1 shows a 3D visualization of a particular realization of a root system generated with the standard input parameter set given in Table 1. Figure 2 shows 3D visualizations of the root systems generated with the minimum and maximum parameter values specified in Table 2. The obtained data sets were then analyzed statistically as described below.

The probability distribution of a random root system measure X is described by n sample values $x_1, ..., x_n$ that can be visualized, e.g., by a histogram. As a first step, we estimated the probability density function f_X of X using a nonparametric approach, namely a kernel density estimator (KDE). A KDE of f_X is defined as

$$\hat{f}_{X,\mathrm{KDE}}(s) = \frac{1}{\lambda n}\sum_{i=1}^{n} K_\lambda(s, x_i)$$

where the Gaussian kernel $K_\lambda(s,x) = \Phi(|x - s|/\lambda)$ is used with $\Phi(s) = (2\pi)^{-1/2}\exp[-(1/2)s^2]$. The bandwidth $\lambda > 0$ is selected using Scott's rule (Scott, 1979). Intuitively, each point s is assigned a value $K_\lambda(s,x_i)$ corresponding to the distance between s and the ith realization x_i of the random root system measure X. The superposition of all these values of every sample forms a KDE. One advantage of a KDE compared with directly investigating the histogram is that it is much easier to get an understanding of the underlying probability distribution because a KDE is not based on discrete bins and produces smooth estimates of the density function. However, being a nonparametric estimator, it does not give the concise representation of a parametric approach.

We account for this in a further step where we fit and compare several types of parametric distributions. An important type of probability distribution is the normal distribution given by the density

$$f(s) = (2\pi\sigma^2)^{-1/2}\exp\left[-\frac{1}{2\sigma^2}(s-\mu)^2\right]$$

with mean μ and variance $\sigma^2 > 0$. Furthermore, for skewed data, several parametric distributions are available. The lognormal distribution is given by $X = \exp(Y)$, where Y denotes a normally

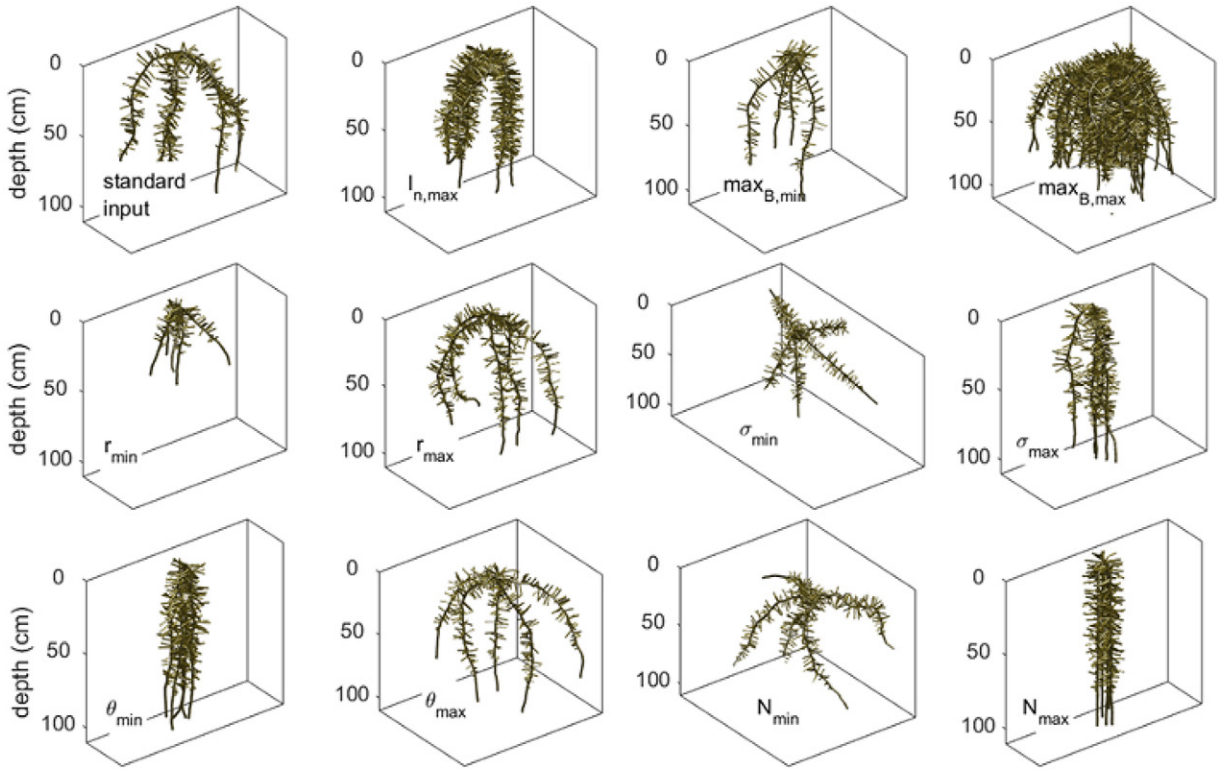

Fig. 2. Three-dimensional visualization of root architectures simulated by CRootBox using the reference parameter set of Table 1 and setting the six input parameters selected for variation—branch spacing (l_n), maximal number of basal roots (max_B), initial elongation rate (r), range of random deflection angle (σ), insertion or branching angle (θ), and number of additional trials (N)—one at a time to minimum and maximum values of the respective parameter range (Table 2).

distributed random variable. Another important example is the γ distribution given by the density

$$f(s)=\exp\left[\frac{-(s-\alpha_\Gamma)}{\theta_\Gamma}\right]\frac{(s-\alpha_\Gamma)^{k_\Gamma-1}}{\Gamma(k_\Gamma)\theta_\Gamma^{k_\Gamma}}$$

for $s > 0$ with shape $k_\Gamma > 0$, scale $\theta_\Gamma > 0$, and location parameter α_Γ, where Γ denotes the gamma function. The inverse gamma distribution is defined as follows: Let Y be gamma distributed, then $X = 1/Y$ is inverse gamma distributed and the density of X is given by

$$f(s)=\frac{\beta_{\Gamma^{-1}}^{\alpha_{\Gamma^{-1}}}}{\Gamma\left(\alpha_{\Gamma^{-1}}\right)}\left(s-\theta_{\Gamma^{-1}}\right)^{-\alpha_{\Gamma^{-1}}-1}\exp\left(\frac{-\beta_{\Gamma^{-1}}}{s-\theta_{\Gamma^{-1}}}\right)$$

with shape $\alpha_{\Gamma^{-1}} > 0$, scale $\beta_{\Gamma^{-1}} > 0$, and location parameter $\theta_{\Gamma^{-1}}$. The parameters of the above (parametric) probability distributions were estimated using the maximum-likelihood method; the type of the parametric distribution was chosen manually by comparing the visual fit of its density to the KDE.

Additionally, so-called Q-Q (quantile–quantile) plots were used to evaluate the goodness of fit. More precisely, a Q-Q plot is a method to visually compare two distributions. Let F_X and F_Y be cumulative distribution functions. The Q-Q plot is then given by $s \to [F_X^{-1}(s), F_Y^{-1}(s)]$ for $s \in (0,1)$, where F^{-1} denotes the inverse function of F, the so-called quantile function. In our case, F_Y is the empirical distribution function of the sample $x = (x_1, ..., x_n)$ and it is thus possible to rewrite the formula above as $i \to [F_X^{-1}(i/n), x_{(i)}]$ for $i = 1, ..., n$, where $x_{(i)}$ is the (standardized) order statistics of the sample x. It is clear that if the two distributions fit perfectly, we get a straight line with a 45° angle. If the Q-Q plot is steeper than this line, then F_Y is more dispersed than F_X and vice versa. This allows us in particular to compare the skewness (S-shape) and the tails of the two distributions graphically. For further information on Q-Q plots, see Gibbons and Chakraborti (2010).

To analyze the dependence of a descriptor z of a root system measure (dependent variable) on an input parameter p (regressor variable), we use polynomial regression models. That is, our model is $z = \beta_0 + \beta_1 p + \beta_2 p^2$. The coefficients β_i are determined by the ordinary least squares method. The decision if a polynomial of degree 1 or 2 is used, i.e., whether β_2 is fixed to be 0, is done manually by maximizing the coefficient of determination R^2, which is computed using leave-one-out cross-validation (Hastie et al., 2009). In our case, for a selected model input parameter, we are mapping its value p, for example, to the mean value $z = (1/n)\Sigma_{i=1}^{n} x_i$ of all realizations $x_1, ..., x_n$ of a root system measure given p.

We have discussed above how descriptors of single root system measures can depend on a given input parameter, but it is also of great interest if and how root system measures depend on each other. For this reason, we consider the sample correlation coefficient

$$\hat{r}(x,y)=\sum_{i=1}^{n}\frac{(x_i-\overline{x})(y_i-\overline{y})}{(n-1)\sqrt{s_x^2 s_y^2}}$$

where $\overline{x}$ and $\overline{y}$ are the sample means and s_x^2 and s_y^2 are the sample variances of $x = x_1, ..., x_n$ and $y = y_1, ..., y_n$. In our case, x and y correspond to samples of two characteristic root system measures X and Y of a given input parameter configuration.

Results and Discussion

All the analyses can be reproduced by using the data in HDF5 format and the Jupyter Notebook, which can be downloaded from our publication archive on the github repository of CRootBox: https://github.com/Plant-Root-Soil-Interactions-Modelling/CRootBox/tree/master/publication%20archive/VZJ%202018. The resulting pdf of the analysis can also be downloaded there.

Due to the large amount of data, we focus here only on selected results; the complete analysis can be found in the Supplemental Material S1: Complete Analysis.pdf (available at https://github.com/Plant-Root-Soil-Interactions-Modelling/CRootBox/tree/master/publication%20archive/VZJ%202018).

Probability Density Functions

All absolute root system measures (i.e., z_{max}, r_{max}, conv, RL, RSA, RV, NR, V_{rhizo}) were approximately normally distributed. The parameters of the fitted normal distributions, however, varied with changing model input parameters. Root measures based on ratios (i.e., RND, RLD, RSAD, RVD, and VD_{rhizo}) were distributed according to the complex distribution function for ratios of correlated normally distributed variables derived by Hinkley (1969). In most cases, they showed skewed probability distributions, which could be well approximated with inverse γ distributions, whose parameters, again, depended on the model input parameterization. This can be illustrated by the example of root tip density (RND): For low values of the maximal number of primary roots (max_B), the probability distribution of RND is strongly positively skewed, while the skewness becomes less for larger values of max_B (Fig. 3). In most cases, the Q-Q plots showed good agreement between sample data and theoretical fit, suggesting that the fitted normal or inverse γ distributions are valid approximations. The probability distributions for all root system measures are provided in the Supplemental Material S1 on github. It follows from the differences in skewness that it is required to correctly sample from these distributions to appropriately represent root system or plant diversity. Otherwise, we could miss some "extreme" root systems that might be the most suited under extreme conditions such as water stress, drought stress, nutrient limitations, etc.

Regressions

Here, we describe and interpret the impact of selected model input parameters on root system measures using the fitted regression models. An overview of the relationships is given in Fig 4. Figure 5 visualizes the dependence of root system measures on model input parameters by means of three examples.

Variations in branch spacing l_n have no influence on root system measures defining the shape of the root system (z_{max}, r_{max}, or conv) but significantly impact total root system size, V_{rhizo}, and root hydraulic architecture measures (K_{rs}, $K_{rs\,L}$, and $K_{rs\,A}$). Absolute measures defining the total size of a root system (RL, RSA, RV, and NR), V_{rhizo}, as well as ratios including these measures (RND, RLD, RSAD, RVD, and VD_{rhizo}) decrease nonlinearly with larger branch spacing. The half mean distance between roots (HMD) increases linearly with greater values of l_n. As expected, K_{rs}, which predominantly depends on the surface of the root system, decreases nonlinearly with greater values of l_n. Measures of unit root system conductance ($K_{rs\,L}$ and $K_{rs\,A}$), however, increase with greater l_n, which is caused by a greater decline rate in K_{rs} than in RL or RSA. Due to the length difference between the apical and basal root zones (the apical root zone is generally longer), which becomes important when laterals are scarce, Z_{SUF} increases nonlinearly with greater values of l_n.

In contrast to branch spacing, variations in the insertion angle θ have no impact on measures defining the total size of a root system (RL, RSA, RV, and NR), V_{rhizo}, or root hydraulic architecture measures (K_{rs}, $K_{rs\,L}$, and $K_{rs\,A}$) but strongly influence the shape of a root system. A greater insertion angle leads to a shallower root system and thus to lower z_{max} and z_{SUF} and larger r_{max}. The volume of the convex hull increases linearly with greater θ. Ratios including a measure describing the total size of the root system as well as conv (RND, RLD, RSAD, RVD, and VD_{rhizo}) decrease nonlinearly with greater θ. A larger insertion angle leads to a more widespread root system and thus also to a larger HMD.

A greater number of axial roots, max_B, leads to a linear increase in measures describing the total size of the root system (RL, RSA, RV, and NR) as well as V_{rhizo}. It also increases the likelihood of single roots growing deeper and spreading wider and thus results in greater Z_{max}, r_{max}, and conv. An increase in z_{SUF} is perceptible, however, not statistically significant. Ratios including conv (RND, RLD, RSAD, RVD, and VD_{rhizo}) increase linearly with increasing max_B. A larger number of axial roots leads to a denser root system and thus to a decrease in HMD. While K_{rs} increases with greater values of max_B, measures of unit root system conductance ($K_{rs\,L}$ and $K_{rs\,A}$) decrease due to a lower growth rate of K_{rs} than of RL or RSA.

Higher initial growth speed, r, leads to increases in root system measures defining the total size of a root system (RL, RSA, RV, and NR) as well as V_{rhizo} and K_{rs}. This increase is nonlinear because root elongation follows a negative exponential function whose initial slope is determined by the initial growth speed and whose asymptote is specified by the maximal root length. Higher values of r also lead to greater z_{max}, r_{max}, conv, and z_{SUF}. Ratios that include both a measure describing the total size of the root system and conv (RND, RLD, RSAD, RVD, and VD_{rhizo}) decrease nonlinearly with increasing values of r. This is caused by a larger growth rate of conv than of root measures describing the

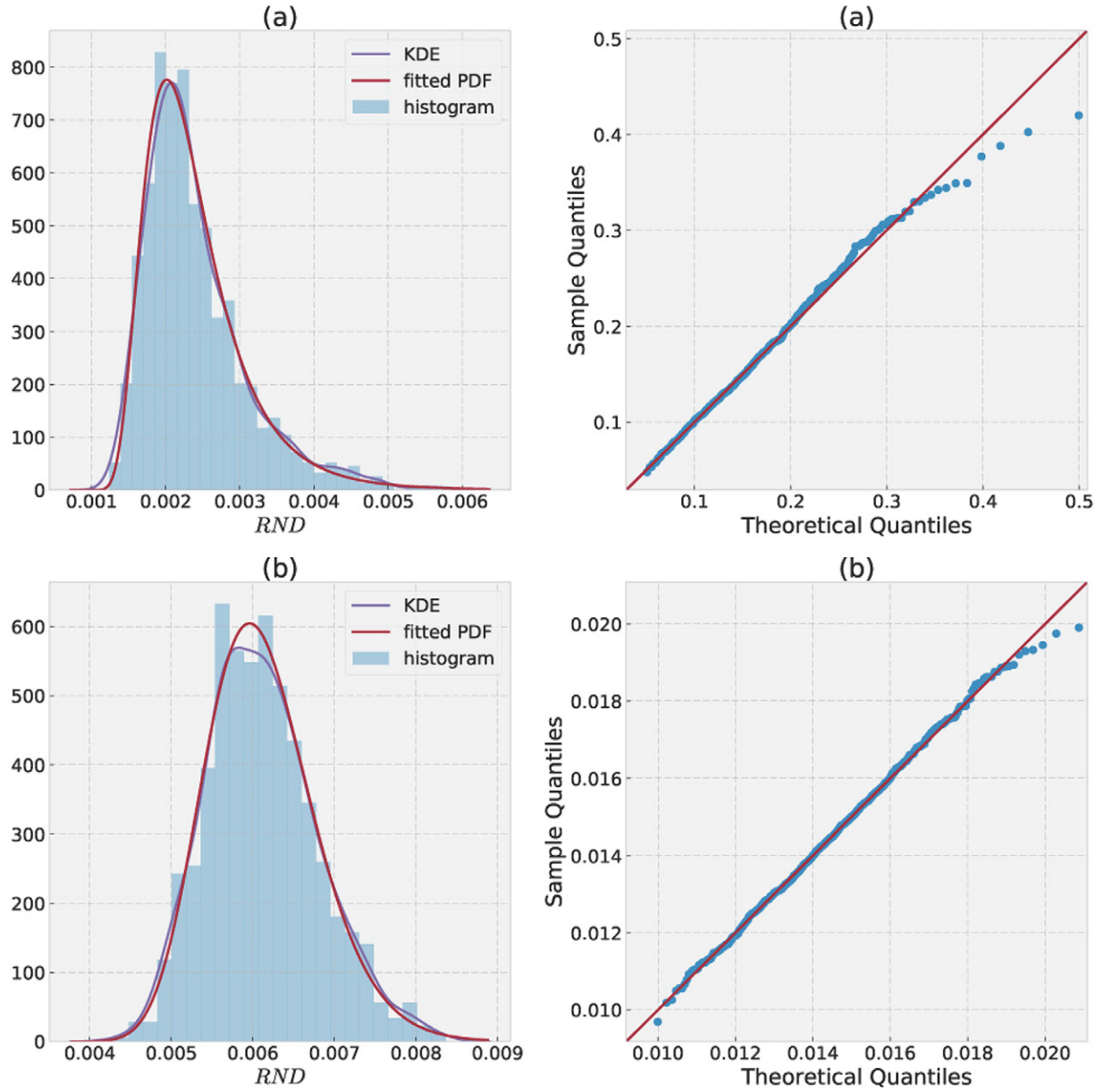

Fig. 3. Contrasting probability density functions, shown as histogram (blue bars), kernel density estimation (KDE, blue line) and fitted parametric model, and Q-Q plots for root tip density at (a) a low number of axial roots (max_B) = 4.0 and (b) a high max_B = 40.0. The parametric model in this case is an inverse gamma distribution with parameters (a) shape $\alpha_{\Gamma^{-1}} = 8.068$, scale $\beta_{\Gamma^{-1}} = 0.01237$, and location $\theta_{\Gamma^{-1}} = 0.0006525$, and (b) $\alpha_{\Gamma^{-1}} = 71.16$, $\beta_{\Gamma^{-1}} = 0.3982$, and $\theta_{\Gamma^{-1}} = 0.0004433$.

size of the root system with increasing r. Greater values of r lead to a larger and thus more widely spread root system, which results in a nonlinear increase of HMD. Again, the growth rate of K_{rs} with greater values of r is lower than that of RL or RSA, which leads to a nonlinear decrease of $K_{rs\,L}$ and $K_{rs\,A}$.

Similar to the insertion angle θ, variations in the range of the random angle deflection σ have no impact on measures defining the total size of a root system (RL, RSA, RV, and NR), on V_{rhizo}, or on root hydraulic architecture parameters (K_{rs}, $K_{rs\,L}$, and $K_{rs\,A}$) but greatly influence the shape of a root system. This influence, however, is complex: greater values of σ lead to both greater root tortuosity and a stronger impact of gravitropism. The way in which variations of σ influence root system measures thus depends on the parameterization of the insertion angle θ as well as on the number of trials N. For $N > 0$ (tropism type *gravitropism*) and $\theta > 1$, greater values of σ increase the probability of vertical reorientation of a root segment and thus lead to higher values of z_{max} and z_{SUF} and lower values of r_{max}. The measures conv and HMD, in contrast, first increase up to a certain threshold value with greater values of σ and then decrease again. This is explained by the predominant influence of tortuosity for smaller values of σ, which leads to a less dense root system. When σ becomes larger, the influence of gravitropism outweighs tortuosity and the root system becomes denser. Ratios including conv

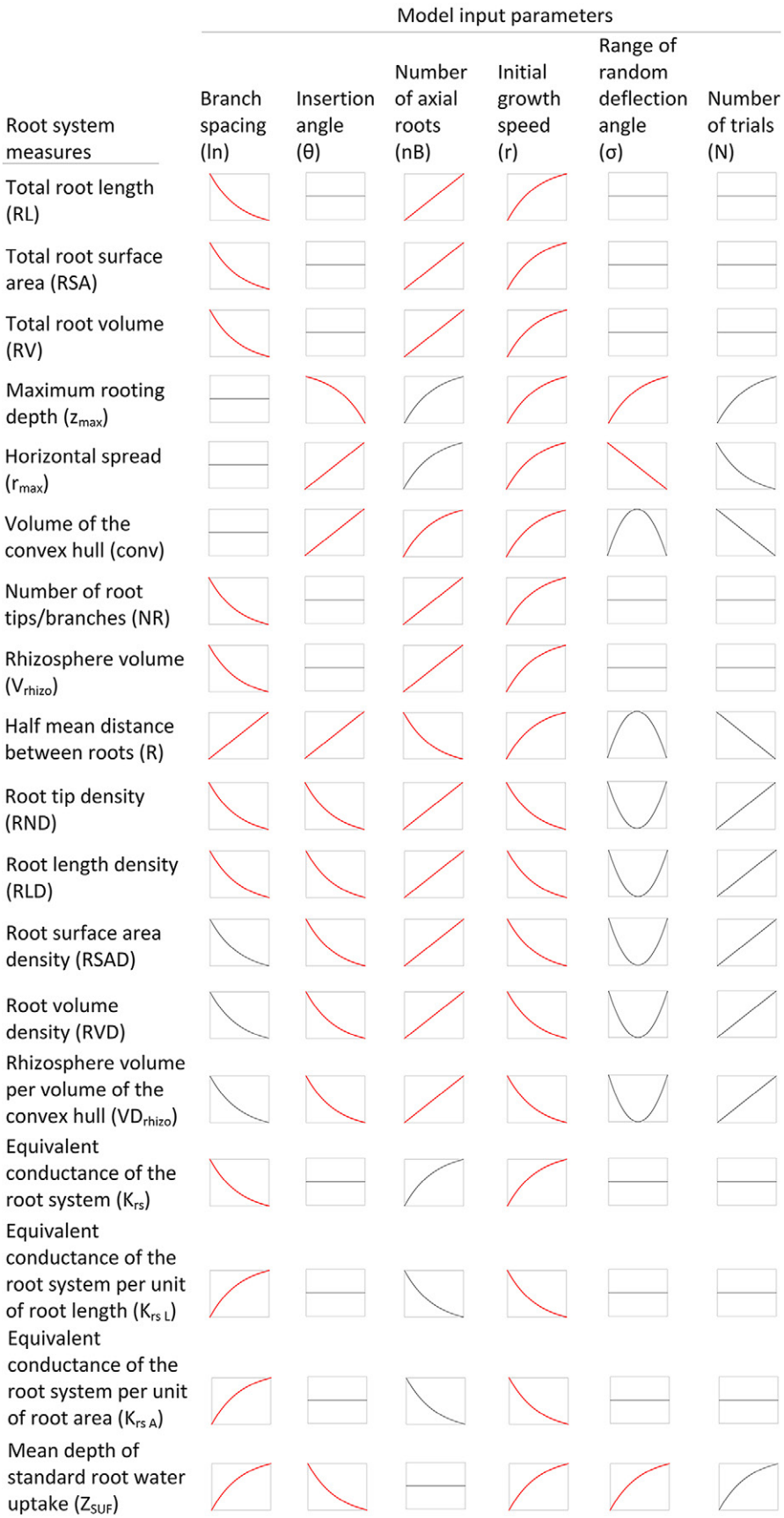

Fig. 4. Dependence between root architecture measures (y axis) and model input parameters (x axis): direct or indirect and linear or nonlinear relationships, respectively, no correlation; regressions with $R^2 > 0.9$ are shown in red.

(RND, RLD, RSAD, RVD, and VD_{rhizo}) as a denominator first decrease to a certain threshold value for increasing values of σ and then increase again.

Variations in the number of trials, N, also do not affect measures defining the total size of a root system (RL, RSA, RV, and NR), V_{rhizo}, or root hydraulic architecture parameters (K_{rs}, $K_{rs\,L}$, and $K_{rs\,A}$) but greatly influence the shape of a root system. A larger N leads to a stronger gravitropic response and thus to higher z_{max} and z_{SUF} and a lower r_{max}. The volume of the convex hull decreases linearly with increasing N. Ratios including a measure describing the total size of the root system as well as the volume of the convex hull (RND, RLD, RSAD, RVD, VD_{rhizo}) increase linearly with increasing N. A larger number of trials leads to a denser root system and thus to a smaller HMD.

Researchers from both plant and soil communities agree that it is important to understand the interactions between roots and soil to better understand plant water and nutrient acquisition (Vetterlein et al., 2018) and soil science (Gregory, 2006). Plant breeding increasingly focuses on roots (Bodner et al., 2015; Lynch, 2007). Wasson et al. (2012), for example, discussed root traits that help increase deep water uptake. They are directly related to the root hydraulic architecture and are included in the set of our model input parameters: axial and radial resistance, maximal root length, and branch spacing. With our approach, it is now possible to quantify the effect of changing both the mean and the variance of those parameters on different root system measures. For example, a deeper root system is postulated as desirable for increased deep water uptake, and two strategies are discussed for achieving this goal: (i) an increased elongation rate of basal roots or (ii) a steeper insertion angle. Figure 4 shows that the mean depth of root water uptake Z_{SUF} increases with increasing insertion angle as well as with increasing elongation rate r. However, increasing r results in an increased root volume RV, while this parameter is not influenced by changing the insertion angle. Taking RV as a proxy for carbon costs, our approach thus is a tool to quantify increased costs associated with strategy (i).

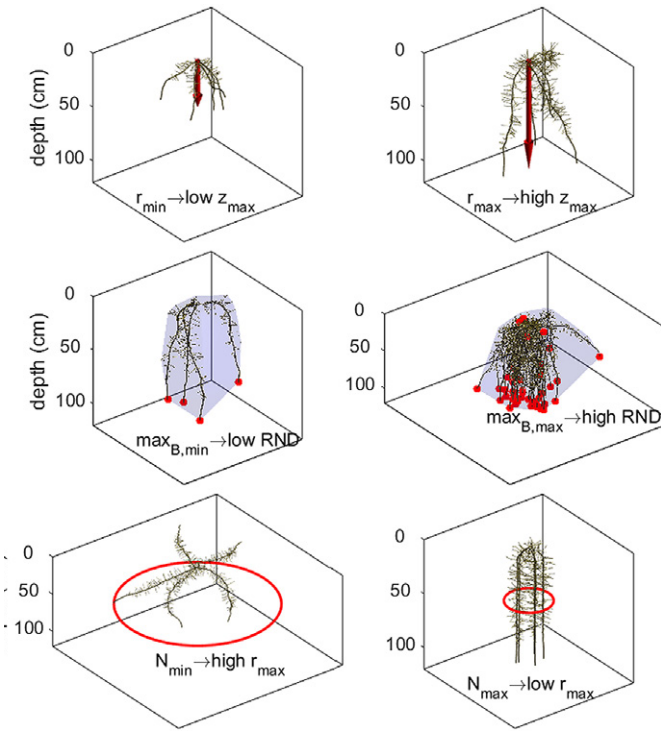

Fig. 5. Three examples visualizing the dependence of root system measures on model input parameters: maximum rooting depth z_{max} as influenced by elongation rate r (top), root tip density RND (number of root tips per convex hull) as influenced by the number of primary roots max_B, where the volume of the convex hull is shown as purple shading and the root tips are indicated by red dots (middle), and maximum horizontal spread r_{max} as influenced by the range of the random angle deflection σ (bottom), with the maximal horizontal spread of the root system indicated by the red circles.

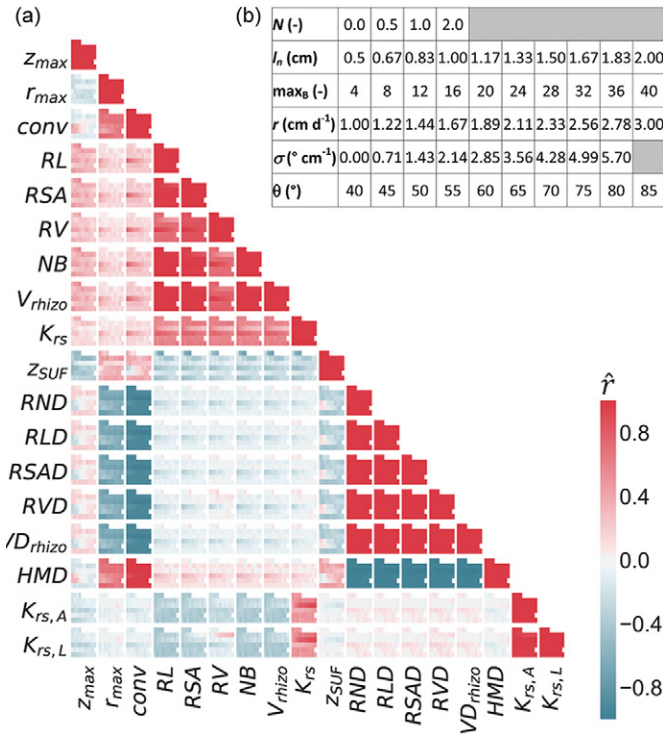

Fig. 6. Correlations between the different root system measures and their variations across the parameter space: (a) the correlation matrix, where each entry is again a matrix in which each line corresponds to one of the selected model input parameters (see Tables 1 and 2), and (b) the small matrix where each color corresponds to the basic model setup in which one parameter was changed according to the value outlined in the small matrix (see Table 3).

Correlations between Different Root System Measures

We quantified correlations between all root system measures. An interesting finding was that some of the correlation coefficients varied across the parameter space. Each entry in the correlation matrix shown in Fig. 6a is again a matrix in which each line corresponds to one of the selected model input parameters and the different values that were chosen for each parameter. Each color in the small matrix thus corresponds to the basic model setup in which one parameter was changed according to the value outlined in the small matrix in Fig. 6b. We observe that all of the density measures (RND, RLD, RSAD, and RVD) have constant strong correlations between each other, irrespective of the chosen parameters. Root surface area density, RSAD, is for example always strongly correlated with the root length density, RLD. In a similar way, the rhizosphere volume is always strongly positive correlated with the root length, whereas there is a constant strongly negative correlation between the half mean distance between roots, HMD, and the densities such as the root length density. As anticipated, maximum horizontal spread and maximum rooting depth are negatively correlated, although the strength of the correlation varies across the parameter space. Such changes in strength of correlation can also be observed for the correlation between equivalent conductance of the root system, K, and the maximum horizontal spread, r_{max}.

Other root system measures show correlations that even change from slightly negative to slightly positive, as in the case of the correlation between the equivalent conductance of the root system per unit root length, $K_{rs\,L}$, and the densities such as RLD, although the correlations are only weak. This makes sense as per the definition of $K_{rs\,L}$, as it is dependent on the root length itself (RL) and not on the soil volume explored by this root system. Consequently, its (negative) correlation with the RL itself is stronger.

In the correlation between the volume of the convex hull, conv, and the maximal rooting depth, z_{max}, we also observe that there are a few parameterizations in which the correlation is positive. In the basic setup, the root system is parameterized such that it shows gravitropism. Hence, as long as the parameter σ is large enough, the root system becomes steeper with time due to gravitropism. This is at the cost of the volume of the convex hull—the steeper the root system, the smaller the convex hull. Hence there is a negative correlation between the maximum rooting depth and the volume of the convex hull. However, if σ is small, then the root system does not show gravitropism, such that an increase in maximum rooting depth will also mean an increase in the volume of the convex hull and thus a positive correlation between conv and z_{max}.

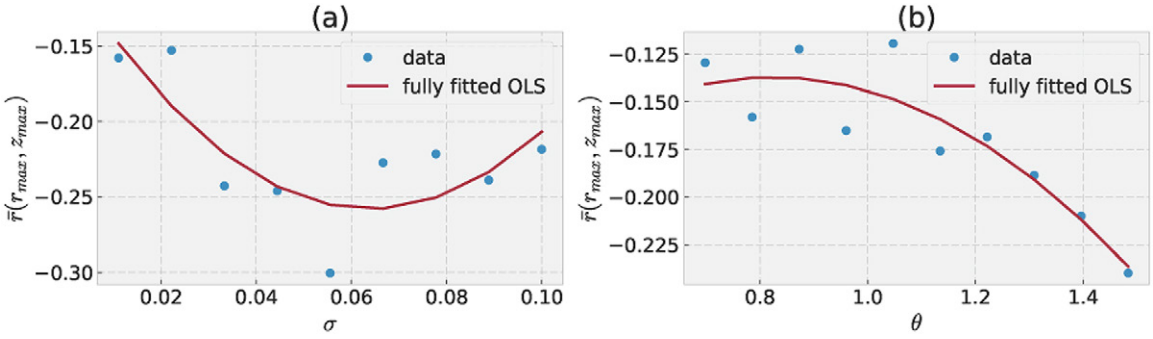

Fig. 7. Correlation determined by ordinary least squares (OLS) fitting between rooting depth (r_{max}) and horizontal spread (z_{max}) as a function of the model input parameters (a) range of random deflection angle σ and (b) insertion or branching angle θ.

Figure 7a shows the nonlinear change in correlation between the maximum rooting depth and horizontal spread with a varying range of the random deflection angle σ, which could be approximated with a quadratic polynomial with a minimum at σ = 0.7. For increasing values of σ below 0.7, the decrease rate in the maximum rooting depth is thus larger than the growth rate in the horizontal spread. For increasing values of σ above 0.7, the decrease rate in the maximum rooting depth is then smaller than the growth rate in the horizontal spread. Figure 7b shows the nonlinear change in correlation between the maximum rooting depth and horizontal spread with a varying range of the insertion angle θ; while the correlation is approximately constant for smaller values of θ, it becomes more negative as θ increases, meaning that the decrease rate in the maximum rooting depth is larger than the growth rate in the horizontal spread with increasing values of θ.

From the point of view of ecology, our modeling and analysis approach provides a tool to predict which model input parameters ("root traits") will or need to be tuned to achieve a given measure in a given environment ("root system trait") and how the link between the two also depends on the parameter variance (see also Landl et al., 2018).

Conclusions

CRootBox is a mechanistic root architecture model with stochastic components. Using statistical methods, we analyzed characteristic root system measures of root systems simulated with CRootBox. We found that absolute root system measures have a normal probability distribution, while ratios of root system measures have an inverse γ distribution. The general shapes of the regression curves that determine the effect of parameter variations on root system measures, as illustrated in Fig. 4, are expected to remain qualitatively similar for other parameterizations. Furthermore, we found that correlations between different root system measures are also variable across the parameter space.

In conclusion, our statistical analysis of the simulation outcome of the 3D root architecture model CRootBox helped to understand the impact of model structure and model parameterization on characteristic root system measures. Other root architecture models use different approaches to describe processes of root system development. The effect of these different approaches on simulated root system measures, however, has never been analyzed systematically. Our presented method can be applied to selected root traits (model input parameters) to achieve a certain outcome (root system measure). It can also be used to compare different root architecture models, including the effects of their stochasticity. And it can be used to compare probability distributions of root system measures obtained from simulations and experimental data (e.g., from 3D root images). Compared with experiments, model simulation can usually be repeated much more often; in this work, the number of replications for each parameter set was 1000. Thus, experimental data could be used to inform and parameterize root architecture models, which can then in turn be used to create realistic, data-driven scenarios for further investigations. The meta-models derived here are simple polynomial regression models. In the future, this work shall be extended to more complex statistical methods including multivariate approaches such as copulas, which provide mathematical tools to build meta-models for vectors of (correlated) root system measures instead of doing this for each individual measure separately.

Supplemental Material

The complete statistical analysis is available as Supplemental Material S1: Complete Analysis.pdf (available at https://github.com/Plant-Root-Soil-Interactions-Modelling/CRootBox/tree/master/publication%20archive/VZJ%202018). It is structured according to the different root system measures considered in this study. For each individual root system measure and input parametrization, a probability density function as well as kernel density estimation (purple line) are plotted. Fitted normal respectively inverse-gamma distributions are represented by a red line. The Q–Q plots show the goodness of fit of the estimated functions. Thereafter, regressions showing the dependency between variations of input parameters and root system measures are presented. Finally, correlations are shown between root system measures and their dependency on variations of input parameters.

Acknowledgments

M. Landl acknowledges funding from the German Research Foundation, DFG, within the research unit DFG PAK 888.

References

Atkinson, J.A., L.U. Wingen, M. Griffiths, M.P. Pound, O. Gaju, M.J. Foulkes, et al. 2015. Phenotyping pipeline reveals major seedling root growth QTL in hexaploid wheat. J. Exp. Bot. 66:2283–2292. doi:10.1093/jxb/erv006

Bingham, I.J., and L. Wu. 2011. Simulation of wheat growth using the 3D root architecture model SPACSYS: Validation and sensitivity analysis. Eur. J. Agron. 34:181–189. doi:10.1016/j.eja.2011.01.003

Bodner, G., D. Leitner, A. Nakhforoosh, M. Sobotik, K. Moder, and H.-P. Kaul. 2013. A statistical approach to root system classification. Front. Plant Sci. 4:292. doi:10.3389/fpls.2013.00292

Bodner, G., A. Nakhforoosh, and H.-P. Kaul. 2015. Management of crop water under drought: A review. Agron. Sustain. Dev. 35:401–442. doi:10.1007/s13593-015-0283-4

Chen, Y., M.E. Ghanem, and K.H. Siddique. 2017. Characterising root trait variability in chickpea (*Cicer arietinum* L.) germplasm. J. Exp. Bot. 68:1987–1999.

Couvreur, V., J. Vanderborght, X. Draye, and M. Javaux. 2014. Dynamic aspects of soil water availability for isohydric plants: Focus on root hydraulic resistances. Water Resour. Res. 50:8891–8906. doi:10.1002/2014WR015608

Couvreur, V., J. Vanderborght, and M. Javaux. 2012. A simple three-dimensional macroscopic root water uptake model based on the hydraulic architecture approach. Hydrol. Earth Syst. Sci. 16:2957–2971. doi:10.5194/hess-16-2957-2012

Doussan, C., A. Pierret, E. Garrigues, and L. Pagès. 2006. Water uptake by plant roots: II. Modelling of water transfer in the soil root-system with explicit account of flow within the root system—Comparison with experiments. Plant Soil 283:99–117.

Dunbabin, V.M., A.J. Diggle, Z. Rengel, and R. van Hugten. 2002. Modelling the interactions between water and nutrient uptake and root growth. Plant Soil 239:19–38. doi:10.1023/A:1014939512104

Garré, S., E. Laloy, M. Javaux, and H. Vereecken. 2012. Parameterizing a dynamic architectural model of the root system of spring barley from minirhizotron data. Vadose Zone J. 11(4). doi:10.2136/vzj2011.0179

Gibbons, J.D., and S. Chakraborti. 2010. Nonparametric statistical inference. 5th ed. CRC Press, Boca Raton, FL.

Gregory, P.J. 2006. Roots, rhizosphere and soil: The route to a better understanding of soil science? Eur. J. Soil Sci. 57:2–12. doi:10.1111/j.1365-2389.2005.00778.x

Hastie, T., R. Tibshirani, and J. Friedman. 2009. The elements of statistical learning. Springer, New York. doi:10.1007/978-0-387-84858-7

Hinkley, D.V. 1969. On the ratio of two correlated normal random variables. Biometrika 56:635–639. doi:10.1093/biomet/56.3.635

Landl, M., A. Schnepf, J. Vanderborght, A.G. Bengough, S.L. Bauke, G. Lobet, et al. 2018. Measuring root system traits of wheat in 2D images to parameterize 3D root architecture models. Plant Soil 425:457–477. doi:10.1007/s11104-018-3595-8

Leitner, D., S. Klepsch, A. Knieß, and A. Schnepf. 2010. The algorithmic beauty of plant roots: An L-system model for dynamic root growth simulation. Math. Comput. Model. Dyn. Syst. 16:575–587. doi:10.1080/13873954.2010.491360

Leitner, D., F. Meunier, G. Bodner, M. Javaux, and A. Schnepf. 2014. Impact of contrasted maize root traits at flowering on water stress tolerance: A simulation study. Field Crops Res. 165:125–137. doi:10.1016/j.fcr.2014.05.009

Lynch, J.P. 2007. Roots of the second Green Revolution. Aust. J. Bot. 55:493–512. doi:10.1071/BT06118

Lynch, J.P. 2013. Steep, cheap and deep: An ideotype to optimize water and N acquisition by maize root systems. Ann. Bot. 112:347–357. doi:10.1093/aob/mcs293

Lynch, J.P., and K.M. Brown. 2001. Topsoil foraging: An architectural adaptation of plants to low phosphorus availability. Plant Soil 237:225–237. doi:10.1023/A:1013324727040

Meunier, F., V. Couvreur, X. Draye, J. Vanderborght, and M. Javaux. 2017a. Towards quantitative root hydraulic phenotyping: Novel mathematical functions to calculate plant-scale hydraulic parameters from root system functional and structural traits. J. Math. Biol. 75:1133–1170. doi:10.1007/s00285-017-1111-z

Meunier, F., X. Draye, J. Vanderborght, M. Javaux, and V. Couvreur. 2017b. A hybrid analytical-numerical method for solving water flow equations in root hydraulic architectures. Appl. Math. Modell. 52:648–663. doi:10.1016/j.apm.2017.08.011

Meunier, F., M. Javaux, V. Couvreur, and X. Draye, and J. Vanderborght. 2016. A new model for optimizing the water acquisition of root hydraulic architectures over full crop cycles. In: International Conference on Functional-Structural Plant Growth Modeling, Simulation, Visualization and Applications (FSPMA), Qingdao, China. 7–11 Nov. 2016. IEEE, New York. p. 140–149. doi:10.1109/FSPMA.2016.7818300

Nagel, K.A., D. Bonnett, R. Furbank, A. Walter, U. Schurr, and M. Watt. 2015. Simultaneous effects of leaf irradiance and soil moisture on growth and root system architecture of novel wheat genotypes: Implications for phenotyping. J. Exp. Bot. 66:5441–5452. doi:10.1093/jxb/erv290

Newman, E.I. 1969. Resistance to water flow in soil and plant: I. Soil resistance in relation to amounts of root—Theoretical estimates. J. Appl. Ecol. 6:1–12. doi:10.2307/2401297

Pagès, L. 2011. Links between root developmental traits and foraging performance. Plant Cell Environ. 34:1749–1760. doi:10.1111/j.1365-3040.2011.02371.x

Pagès, L., C. Bécel, H. Boukcim, D. Moreau, C. Nguyen, and A.-S. Voisin. 2014. Calibration and evaluation of ArchiSimple, a simple model of root system architecture. Ecol. Modell. 290:76–84. doi:10.1016/j.ecolmodel.2013.11.014

Pagès, L., G. Vercambre, J.-L. Drouet, F. Lecompte, C. Collet, and J. Le Bot. 2004. Root Typ: A generic model to depict and analyse the root system architecture. Plant Soil 258:103–119. doi:10.1023/B:PLSO.0000016540.47134.03

Poorter, H., F. Fiorani, R. Pieruschka, T. Wojciechowski, W.H. Putten, M. Kleyer, et al. 2016. Pampered inside, pestered outside? Differences and similarities between plants growing in controlled conditions and in the field. New Phytol. 212:838–855. doi:10.1111/nph.14243

Postma, J.A., C. Kuppe, M.R. Owen, N. Mellor, M. Griffiths, M.J. Bennett, et al. 2017. OpenSimRoot: Widening the scope and application of root architectural models. New Phytol. 215:1274–1286. doi:10.1111/nph.14641

Postma, J.A., and J.P. Lynch. 2011. Root cortical aerenchyma enhances the growth of maize on soils with suboptimal availability of nitrogen, phosphorus, and potassium. Plant Physiol. 156:1190–1201. doi:10.1104/pp.111.175489

Schnepf, A., D. Leitner, M. Landl, G. Lobet, T.H. Mai, S. Morandage, et al. 2018. CRootBox: A structural–functional modelling framework for root systems. Ann. Bot. 121:1033–1053. doi:10.1093/aob/mcx221

Scott, D.W. 1979. On optimal and data-based histograms. Biometrika 66:605–610. doi:10.1093/biomet/66.3.605

Vadez, V. 2014. Root hydraulics: The forgotten side of roots in drought adaptation. Field Crops Res. 165:15–24. doi:10.1016/j.fcr.2014.03.017

van Noordwijk, M., J. Floris, and A. de Jager. 1985. Sampling schemes for estimating root density distribution in cropped fields. Neth. J. Agric. Sci. 33:241–262.

Vetterlein, D., S. Schlüter, and H.-J. Vogel. 2018. Root systems offer insight into better soils. Nature 554:423. doi:10.1038/d41586-018-02202-y

Wasson, A.P., R.A. Richards, R. Chatrath, S.C. Misra, S.V. Sai Prasad, G.J. Rebetzke, et al. 2012. Traits and selection strategies to improve root systems and water uptake in water-limited wheat crops. J. Exp. Bot. 63:3485–3498. doi:10.1093/jxb/ers111

Wojciechowski, T., M.J. Gooding, L. Ramsay, and P.J. Gregory. 2009. The effects of dwarfing genes on seedling root growth of wheat. J. Exp. Bot. 60:2565–2573. doi:10.1093/jxb/erp107

Zhang, B.G., P. De Reffye, L. Liu, M.Z. Kang, and B.G. Li. 2003. Analysis and modeling of the root system architecture of winter wheat seedlings. In: G.-H. Bao and M. Jaeger, editors, Plant Growth Modeling and Applications: Proceedings of the International Symposium on Plant Growth Modeling, Simulation, Visualization and their Applications (PMA03), Beijing. October 2003. Tsinghua Univ. Press, Beijing. p. 321–328.

Zuo, Q., F. Jie, R. Zhang, and L. Meng. 2004. A generalized function of wheat's root length density distributions. Vadose Zone J. 3:271–277. doi:10.2136/vzj2004.2710